CLUSTER MAGNETIC FIELDS

C. L. Carilli and G. B. Taylor

National Radio Astronomy Observatory, Socorro, New Mexico 87801;
email: ccarilli@nrao.edu, gtaylor@nrao.edu

Key Words   galaxy clusters, intergalactic medium, intracluster medium, cosmic
rays, observations: radio, x-ray

■ **Abstract**   Magnetic fields in the intercluster medium have been measured using
a variety of techniques, including studies of synchrotron relic and halo radio sources
within clusters, studies of inverse Compton X-ray emission from clusters, surveys of
Faraday rotation measures of polarized radio sources both within and behind clusters,
and studies of cluster cold fronts in X-ray images. These measurements imply that most
cluster atmospheres are substantially magnetized, with typical field strengths of order 1
μGauss with high areal filling factors out to Mpc radii. There is likely to be considerable
variation in field strengths and topologies both within and between clusters, especially
when comparing dynamically relaxed clusters to those that have recently undergone
a merger. In some locations, such as the cores of cooling flow clusters, the magnetic
fields reach levels of 10–40 μG and may be dynamically important. In all clusters the
magnetic fields have a significant effect on energy transport in the intracluster medium.
We also review current theories on the origin of cluster magnetic fields.

INTRODUCTION

Magnetic fields play an important role in virtually all astrophysical phenomena.
Close to home, the Earth has a bipolar magnetic field with a strength of 0.3 G at the
equator and 0.6 G at the poles. This field is thought to originate in a dynamo owing to
fluid motions within the liquid core (Soward 1983). With its faster angular rotation,
Jupiter leads the planets with an equatorial field strength of ∼4 G (Warwick 1963,
Smith et al. 1974). A similar mechanism produces the solar magnetic fields that give
rise to spectacular sunspots, arches, and flares (Parker 1979). Within the interstellar
medium, magnetic fields are thought to regulate star formation via the ambipolar
diffusion mechanism (Spitzer 1978). Our own Galaxy has a typical interstellar
magnetic field strength of ∼2 μG in a regular ordered component on kiloparsec
scales, and a similar value in a smaller scale, random component (Beck et al.
1996, Kulsrud 1999). Other spiral galaxies have been estimated to have magnetic
field strengths of 5 to 10 μG, with fields strengths up to 50 μG found in starburst
galaxy nuclei (Beck et al. 1996). Magnetic fields are fundamental to the observed
properties of jets and lobes in radio galaxies (Bridle & Perley 1984), and they
may be primary elements in the generation of relativistic outflows from accreting,

319

massive black holes (Begelman et al. 1984). Assuming equipartition conditions apply, magnetic field strengths range from a few μG in kpc-scale extended radio lobes, to mG in pc-scale jets.

The newest area of study of cosmic magnetic fields is on even larger scales still, those of clusters of galaxies. Galaxy clusters are the largest virialized structures in the universe. The first spatially resolving X-ray observations of clusters in the early 1970s (e.g., Forman et al. 1972) revealed atmospheres of hot gas (10^7 to 10^8 K) that extend to Mpc radii and that dominate the baryonic mass of the systems (10^{13} to 10^{14} M$_\odot$). Soon thereafter came the first attempts to measure magnetic field strengths in the intercluster medium (ICM) (Jaffe 1977). Only in the last decade has it become clear that magnetic fields are ubiquitous in cluster atmospheres, certainly playing a critical role in determining the energy balance in cluster gas through their effect on heat conduction, and in some cases, perhaps even becoming dynamically important.

Cluster magnetic fields have been treated as secondary topics in reviews of cluster atmospheres (Sarazin 1988, Fabian 1994) and in general reviews of cosmic magnetic fields (Kronberg 1996, Ruzmaikin et al. 1987). To date there has been no dedicated review of cluster magnetic fields.

The focus of this review is primarily observational. We summarize and critique various methods used for measuring cluster magnetic fields. In the course of the review, we consider important effects of magnetic fields in clusters, such as their effect on heat conduction and gas dynamics, and other issues such as the lifetimes of relativistic particles in the ICM. We then attempt to synthesize the various measurements and develop a general picture for cluster magnetic fields, with the caveat that there may be significant differences between clusters, and even within a given cluster atmosphere. We conclude with a section on the possible origin of cluster magnetic fields.

We assume H$_0 = 75$ km s^{-1} Mpc^{-1} and q$_0 = 0.5$, unless stated otherwise. Spectral index, α, is defined as $S_\nu \propto \nu^\alpha$.

SYNCHROTRON RADIATION

Radio Halos

Over 40 years ago, Large (1959) discovered a radio source in the Coma cluster that was extended even when observed with a 45′ beam. This source (Coma C) was studied by Willson (1970) who found that it had a steep spectral index and could not be made up of discrete sources, but instead was a smooth "radio halo" with no structure on scales less than 30′. Willson further surmised that the emission mechanism was likely to be synchrotron, and if in equipartition required a magnetic field strength of 2 μG. In Figure 1, we show the best image yet obtained of the radio halo in the Coma cluster. Other radio halos were subsequently discovered, although the number known remained under a dozen until the mid-1990s (Hanisch 1982).
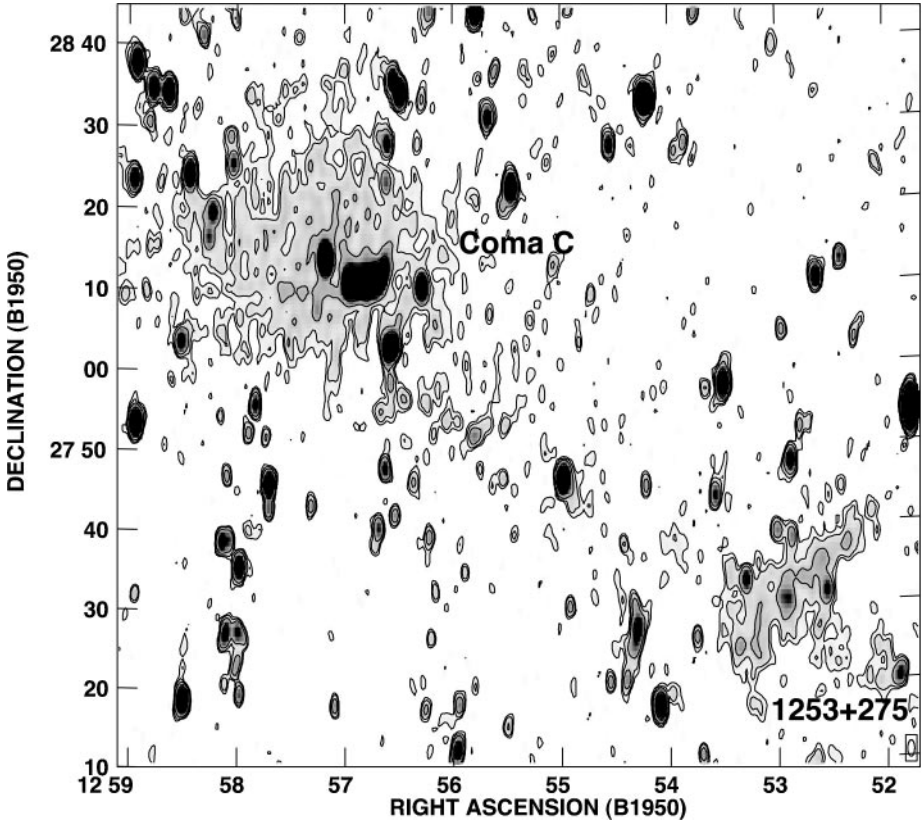
Figure 1   Westerbork Synthesis Radio Telescope (WSRT) radio image of the Coma cluster region at 90 cm, with angular resolution of $55'' \times 125''$ (HPBW, RA $\times$ DEC) for the radio telescope from Feretti & Giovannini (1998). Labels refer to the halo source Coma C and the relic source $1253 + 275$. The gray-scale range displays total intensity emission from 2 to 30 mJy/beam, whereas contour levels are drawn at 3, 5, 10, 30, and 50 mJy/beam. The bridge of radio emission connecting Coma C to $1253 + 275$ is resolved and visible only as a region with an apparent higher positive noise. The Coma cluster is at a redshift of 0.023, such that $1' = 26$ kpc for $H_0 = 75$.

Using the Northern VLA Sky Survey [NVSS (Condon et al. 1998)] and X-ray selected samples as starting points, Giovannini & Feretti (2000) and Giovannini et al. (1999) have performed moderately deep VLA observations (integrations of a few hours) that have more than doubled the number of known radio halo sources. Several new radio halos have also been identified from the Westerbork Northern Sky Survey (Kemper & Sarazin 2001). These radio halos typically have sizes $\sim$1 Mpc, steep spectral indices ($\alpha < -1$), low fractional polarizations ($<$5%), low

surface brightnesses ($\sim 10^{-6}$ Jy arcsec^{-2} at 1.4 GHz), and centroids close to the cluster center defined by the X-ray emission.

A steep correlation between cluster X-ray and radio halo luminosity has been found, as well as a correlation between radio and X-ray surface brightnesses in clusters (Liang et al. 2000, Feretti et al. 2001, Govoni et al. 2001a). A complete (flux limited) sample of X-ray clusters shows only 5% to 9% of the sources are detected at the surface brightness limits of the NVSS of 2.3 mJy beam^{-1}, where the beam has FWHM $= 45''$ (Giovannini & Feretti 2000, Feretti et al. 2001). But this sample contains mostly clusters with X-ray luminosities $<10^{45}$ erg s^{-1}. If one selects for clusters with X-ray luminosities $>10^{45}$ erg s^{-1}, the radio detection rate increases to 35% (Feretti et al. 2001, Owen et al. 1999). Likewise, there may be a correlation between the existence of a cluster radio halo and the existence of substructure in X-ray images of the hot cluster atmosphere, indicative of merging clusters, and a corresponding anticorrelation between cluster radio halos and clusters with relaxed morphologies, e.g., cooling flows (Govoni et al. 2001a), although these correlations are just beginning to be quantified (Buote 2001).

Magnetic fields in cluster radio halos can be derived, assuming a minimum energy configuration for the summed energy in relativistic particles and magnetic fields (Burbidge 1959), corresponding roughly to energy equipartition between fields and particles. The equations for deriving minimum energy fields from radio observations are given in Miley (1980). Estimates for minimum energy magnetic field strengths in cluster halos range from 0.1 to 1 μG (Feretti 1999). One of the best studied halos is that in Coma, for which Giovannini et al. (1993) report a minimum energy magnetic field of 0.4 μG. These calculations typically assume $k = 1$, $\eta = 1$, $\nu_{low} = 10$ MHz, and $\nu_{high} = 10$ GHz, where k is the ratio of energy densities in relativistic protons to that in electrons, η is the volume filling factor, ν_{low} is the low frequency cut-off for the integral, and ν_{high} is the high frequency cut-off. All of these parameters are poorly constrained, although the magnetic field strength only behaves as these parameters raised to the $\frac{2}{7}$ power. For example, using a value of $k \sim 50$, as observed for Galactic cosmic rays (Meyer 1969), increases the fields by a factor of three.

Brunetti et al. (2001a) present a method for estimating magnetic fields in the Coma cluster radio halo independent of minimum energy assumptions. They base their analysis on considerations of the observed radio and X-ray spectra, the electron inverse Compton and synchrotron radiative lifetimes, and reasonable mechanisms for particle reacceleration. They conclude that the fields vary smoothly from 2 ± 1 μG in the cluster center, to 0.3 ± 0.1 μG at 1 Mpc radius.

Radio Relics

A possibly related phenomena to radio halos is a class of sources found in the outskirts of clusters known as radio relics. Like the radio halos, these are very extended sources without an identifiable host galaxy (Figure 1). Unlike radio halos, radio relics are often elongated or irregular in shape, are located at the cluster

periphery (by definition), and are strongly polarized [up to 50% in the case of the relic $0917 + 75$ (Harris et al. 1993)]. As the name implies, one of the first explanations put forth to explain these objects was that these are the remnants of a radio jet associated with an active galactic nucleus (AGN) that has since turned off and moved on. A problem with this model is that, once the energy source is removed, the radio source is expected to fade on a timescale $\ll 10^8$ years due to adiabatic expansion, inverse Compton, and synchrotron losses (see "Electron Lifetimes" below). This short timescale precludes significant motion of the host galaxy from the vicinity of the radio source.

A more compelling explanation is that the relics are the result of first order Fermi acceleration (Fermi I) of relativistic particles in shocks produced during cluster mergers (Ensslin et al. 1998), or are fossil radio sources revived by compression associated with cluster mergers (Ensslin & Gopal-Krishna 2001, Röttgering et al. 1994). Equipartition field strengths for relics range from 0.4–3.0 μG (Ensslin et al. 1998). If the relics are produced by shocks or compression during a cluster merger, then Ensslin et al. (1998) calculate a pre-shock cluster magnetic field strength in the range 0.2–0.5 μG.

FARADAY ROTATION

Cluster Center Sources

The presence of a magnetic field in an ionized plasma sets a preferential direction for the gyration of electrons, leading to a difference in the index of refraction for left versus right circularly polarized radiation. Linearly polarized light propagating through a magnetized plasma experiences a phase shift of the left versus right circularly polarized components of the wavefront, leading to a rotation of the plane of polarization, $\Delta \chi = \text{RM} \lambda^2$, where $\Delta \chi$ is the change in the position angle of polarization, λ is the wavelength of the radiation, and RM is the Faraday rotation measure. The RM is related to the thermal electron density, n_e, and the magnetic field, **B**, as:

$$\text{RM} = 812 \int_0^L n_e \mathbf{B} \cdot d\mathbf{l} \, \text{radians m}^{-2}, \tag{1}$$

where **B** is measured in μGauss, n_e in cm^{-3} and $d\mathbf{l}$ in kpc, and the boldface symbols represent the vector product between the magnetic field and the direction of propagation. This phenomenon can also be understood qualitatively by considering the forces on the electrons.

Synchrotron radiation from cosmic radio sources is well known to be linearly polarized, with fractional polarizations up to 70% in some cases (Pacholczyk 1970). Rotation measures (RM) can be derived from multifrequency polarimetric observations of these sources by measuring the position angle of the polarized radiation as a function of frequency. The RM values can then be combined with

measurements of n_e to estimate the magnetic fields. Due to the vector product in Equation 1, only the magnetic field component along the line-of-sight is measured, so the results depend on the assumed magnetic field topology.

Most extragalactic radio sources exhibit Faraday rotation measures (RMs) of the order of tens of rad m^{-2} due to propagation of the emission through the interstellar medium of our galaxy (Simard-Normandin et al. 1981). Sources at Galactic latitudes $\leq 5°$ can exhibit $\sim$300 rad m^{-2}. For the past 30 years, however, a small number of extragalactic sources were known to have far higher RMs than could be readily explained as Galactic in origin. Large intrinsic RMs were suspected, but the mechanism(s) producing them were unclear.

Mitton (1971) discovered that the powerful radio galaxy Cygnus A had large and very different RMs (35 versus -1350 rad m^{-2}), in its two lobes (see also Alexander et al. 1984). Whereas its low galactic latitude (5.8°) could possibly be invoked to explain the high RMs, the large difference in RMs over just 2′ was difficult to reproduce in the context of Galactic models. This "RM anomaly" was clarified when Dreher et al. (1987) performed the first high resolution RM studies with the VLA and found complex structure in the RM distribution on arcsec scales (Figure 2), with gradients as large as 600 rad m^{-2} arcsec^{-1}. These large gradients conclusively ruled out a Galactic origin for the large RMs.

Perhaps just as important as the observed RM structure across the lobes of Cygnus A was the discovery that the observed position angles behave quadratically with wavelength to within very small errors over a wide range in wavelengths (Dreher et al. 1987). Examples of this phenomenon are shown in (Figure 5). Moreover, the change in position angle from short to long wavelengths is much larger than π radians in many cases, whereas the fractional polarization remains constant. This result is critical for interpreting the large RMs for cluster center radio sources, providing proof that the large RMs cannot be due to thermal gas mixed with the radio emitting plasma (Dreher et al. 1987). Such mixing would lead to rapid depolarization with increasing wavelength and departures from a quadratic behavior of χ with wavelength (Burn 1966).

The Cygnus A observations were the first to show that the large RMs must arise in an external screen of magnetized, ionized plasma, but cannot be Galactic in origin. Dreher et al. (1987) considered a number of locations for the Faraday screen toward Cygnus A, and concluded that the most likely site was the X-ray emitting cluster atmosphere enveloping the radio source (Fabbiano et al. 1979). They found that magnetic fields in the cluster gas of 2–10 μG could produce the observed RMs.

Since the ground-breaking observations of Cygnus A, RM studies of cluster center radio sources have become a standard tool for measuring cluster fields. RM studies of radio galaxies in clusters can be divided into studies of cooling-flow and noncooling-flow clusters. Cooling-flow clusters are those in which the X-ray emission is strongly peaked at the center, leading to high densities, and cooling times of the hot ICM in the inner $\sim$100 kpc of much less than the Hubble time. To maintain hydrostatic equilibrium, an inward flow may be required (Fabian et al. 1991). Typical mass cooling flow rates are 100 M$_\odot$ yr^{-1}. The actual presence

of material "cooling" and "flowing" is a topic that is hotly debated at present (Binney 2002). What is more agreed upon is that cooling-flow clusters are more dynamically relaxed than noncooling-flow clusters, which often show evidence of cluster mergers (T. Markovic, J.A. Eilek, unpublished manuscript).

Radio galaxies in cooling-flow clusters attracted some of the first detailed RM studies by virtue of their anomalously high RMs [e.g., A1795 (Ge & Owen 1993), Hydra A (Taylor & Perley 1993)]. Out of a sample of 14 cooling-flow clusters with strong embedded radio sources, Taylor et al. (1994, 2001b) found that 10/14 display RMs in excess of $800 \, \mathrm{rad \, m^{-2}}$, two (PKS 0745-191 and 3C 84 in Abell 426) could not be measured due to a lack of polarized flux, and two [Abell 119 (Feretti et al. 1999) and 3C 129 (Taylor et al. 2001a)] that have lower RMs, but with better X-ray observations, turn out not to be in cooling-flow clusters. Hence, current data are consistent with all radio galaxies at the center of cooling-flow clusters having extreme RMs, with the magnitude of the RMs roughly proportional to the cooling-flow rate (see Figure 3).

The RM distributions for radio sources found at the centers of cooling-flow clusters tend to be patchy with coherence lengths of 5–10 kpc (Figure 4). Larger "patches" up to 30 kpc are seen, for example, in Cygnus A (Figure 2). In both Cygnus A and Hydra A one can find "bands" of alternating high and low RM (see Figures 2 and 4). Such bands are also found in the noncooling-flow cluster sources (Eilek & Owen 2002), along with slightly larger coherence lengths of 15–30 kpc. In Hydra A, there is a strong trend for all the RMs to the north of the nucleus to be positive and, to the south, negative. To explain this requires a field reversal and implies a large-scale (100 kpc) ordered component to the cluster magnetic fields in Hydra A. Taylor & Perley (1993) found the large-scale field strength to be $\sim 7 \, \mu\mathrm{G}$ and more tangled fields to have a strength of $\sim 40 \, \mu\mathrm{G}$. A similar RM sign reversal across the nucleus is seen in A1795, although in this case the radio source is only 11 kpc in extent.

Minimum cluster magnetic field strengths can be estimated by assuming a constant magnetic field along the line-of-sight through the cluster. Such estimates usually lead to magnetic field strengths of 5 to $10 \, \mu\mathrm{G}$ in cooling-flow clusters, and a bit less (factor ~ 2) in the noncooling-flow clusters.

From the patchiness of the RM distributions it is clear that the magnetic fields are not regularly ordered on cluster (Mpc) scales, but have coherence scales between 5 and 10 kpc. Beyond measuring a mean line-of-site field, the next level of RM modeling entails cells of constant size and magnetic field strength, but random magnetic field direction, uniformly filling the cluster. The RM produced by such a screen will be built up in a random-walk fashion and will thus have an average value of $0 \, \mathrm{rad \, m^{-2}}$, but a dispersion in the RM, σ_{RM}, that is proportional to the square root of the number of cells along the line-of-sight through the cluster. The most commonly fit form to the X-ray observations to obtain the radial electron density distribution, $n_e(r)$, through a cluster is the modified King model (Cavaliere & Fusco-Femiano 1976):

$$n_e(r) = n_0 \left(1 + r^2/r_{\mathrm{c}}^2\right)^{-3\beta/2}, \qquad (2)$$
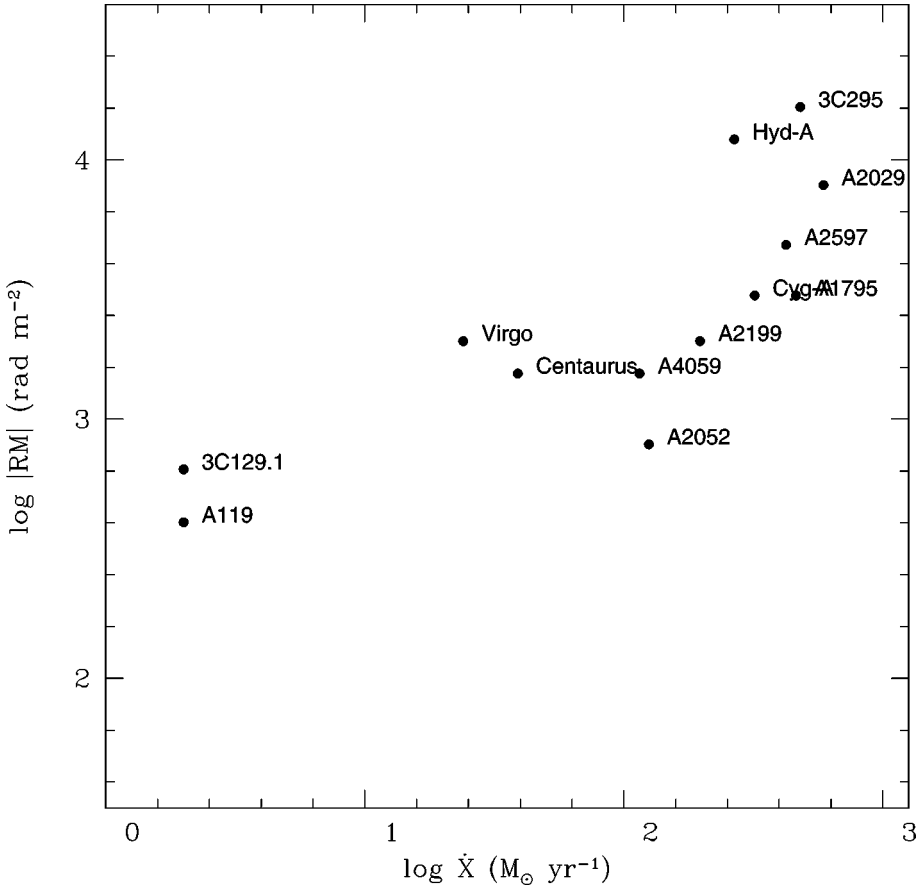
Figure 3   The maximum absolute RM plotted as a function of the estimated cooling flow rate, $\dot{X}$, for a sample of X-ray luminous clusters with measured RMs from Taylor et al. (2002). Both RM and $\dot{X}$ are expected to depend on density to a positive power, so in that sense, the correlation is expected.

where n_0 is the central density, r_c is the core radius, and β is a free parameter in the fit. Typical values for these parameters are $r_c \sim 200$ kpc, $\beta \sim \frac{2}{3}$, and $n_o \sim 0.01$ cm^{-3}.

For this density profile and cells of constant magnetic strength but random orientation, Felten (1996) and Feretti et al. (1995) derived the following relation for the RM dispersion:

$$\sigma_{\mathrm{RM}} = \frac{K B\, n_0\, r_c^{1/2} l^{1/2}}{\left(1 + r^2/r_c^2\right)^{(6\beta-1)/4}} \sqrt{\frac{\Gamma(3\beta - 0.5)}{\Gamma(3\beta)}}, \qquad (3)$$
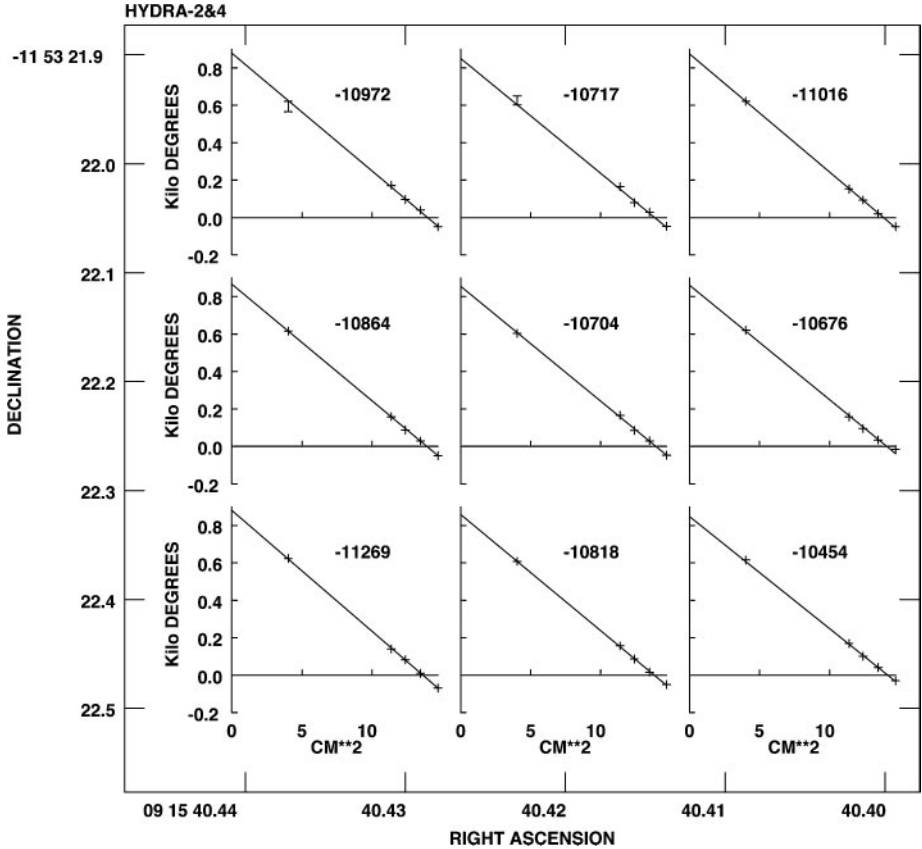
Figure 5 The observed position angles, χ, of the linearly polarized radio emission as a function of the square of the observing wavelength, λ^2, for a number of positions in the southern lobe of Hydra A at a resolution of 0.3″ (Taylor & Perley 1993). The points plotted are each separated by approximately one beamwidth and thus are independent of each other. This illustrates the consistency of the RMs within a coherence length of $\sim$7 kpc. Notice also the excellent agreement to a λ^2-law for $\Delta\chi = 600$ degrees, nearly two complete turns.

where l is the cell size in kpc, r is the distance of the radio source from the cluster center, also in kpc, Γ is the Gamma function, and K is a factor that depends on the location of the radio source along the line-of-sight through the cluster: K = 624 if the source is beyond the cluster, and K = 441 if the source is halfway through the cluster. Note that Equation 3 assumes that the magnetic field strength, B, is related to the component along the line of sight, $(B_{||})$, by $B = \sqrt{3}B_{||}$. The cell size, l, can be estimated to first order from the observed coherence lengths of the RM distributions. Both cooling-flow and noncooling-flow clusters yield typical estimates of 5 to 10 kpc. Magnetic field strength estimates, however are two to

three times higher in the cooling-flow clusters—19 μG in the 3C 295 cluster (Perley & Taylor 1991, Allen et al. 2001a) compared to 6 μG in the 3C 129 cluster (Taylor et al. 2001a) using the methodology described above.

Most radio sources found embedded in clusters are located at the center and identified with a cD galaxy. This relatively high pressure environment has been found in many cases to confine or distort the radio galaxy (Taylor et al. 1994), as well as giving rise to extreme RMs. For this same reason, the extended radio sources in Hydra A and Cygnus A are unique in that they sample regions over 100 kpc in linear extent. There are, however, a few clusters containing more than one strong, polarized radio source. The cluster Abell 119 (Feretti et al. 1999) contains three radio galaxies. Using an analysis based on Equation 3 above, Feretti et al. (1999) find that a magnetic field strength of 6–12 μG extending over 3 Mpc could explain the RM distributions for all 3 sources, although they note that such a field would exceed the thermal pressure in the outer parts of the cluster. In a reanalysis of the Abell 119 measurements, Dolag et al. (2001) find that the field scales as $n_e^{0.9}$. This power-law behavior is marginally steeper than that expected assuming flux conservation, for which the tangled field scales as $n_e^{2/3}$, and significantly steeper than that expected assuming a constant ratio between magnetic and thermal energy density, for which the tangled field scales as $n_e^{1/2}$ for an isothermal atmosphere. In the 3C 129 cluster, there are two extended radio galaxies whose RM observations can be fit by a field strength of 6 μG. Finally, in A514, Govoni et al. (2001a) has measured the RM distributions of five embedded (and background) radio sources and found cluster magnetic field strengths of 4–9 μG spread over the central 1.4 Mpc of the cluster. If the magnetic field scales with the density raised to a positive power, then the product of B and n_e in Equation 1 implies that the observed rotation measures are heavily weighted by the innermost cells in the cluster (Dreher et al. 1987).

It has been suggested that high RMs may result from an interaction between the radio galaxy and the ICM, such that the RMs are generated locally and are not indicative of cluster magnetic fields. Bicknell et al. (1990) proposed a model in which the RM screen is due to a boundary layer surrounding the radio source in which the large magnetic fields within the radio source are mixed with the large thermal densities outside the radio source by Kelvin-Helmholtz waves along the contact discontinuity. This model predicts a Faraday depolarized region of a few kpc extent surrounding the radio source, where the synchrotron emitting material has mixed with the thermal gas. Such a depolarized shell has not been observed to date.

In general, extreme RMs have been observed in sources of very different morphologies, from edge-brightened [Fanaroff-Riley Class II (FR) (Fanaroff & Riley 1974)], to edge-darkened (FR I) sources. The models for the hydrodynamic evolution of these different classes of sources are thought to be very different, with the FR II sources expanding supersonically, whereas the FR I sources expand subsonically (Begelman et al. 1984). The different dynamics of FR I and FR II sources argues that the high RMs are not solely a phenomenon arising from a local

interaction between the radio source and its environment, but are more likely to be a property of the large-scale (i.e., cluster) environment.

Although we feel that large RMs for cluster center radio sources most likely arise in the large-scale cluster atmosphere, we should point out that there are some cases in which the radio source does appear to compress the gas and fields in the ICM to produce local RM enhancements. For example, there is evidence for an RM enhancement at the bow shock preceding the radio hot spots in Cygnus A and 3C 194 (Carilli et al. 1988, Taylor et al. 1992). However, even in these cases, the implied external (i.e., unperturbed) ICM fields are a few μG.

Background and Embedded Sources

The first successful demonstration of Faraday rotation of the polarized emission from background radio sources seen through a cluster atmosphere was presented by Vallee et al. (1986) for A2319. Vallee et al. (1987) combined the RM excess in A2319 with density estimates from X-ray observations by Jones et al. (1979) to estimate a field strength of 2 μG if the field is organized in 20 kpc-sized cells. Hennessy et al. (1989) studied a sample of 16 sources located behind Abell clusters and found no significant RM excess compared to a control sample of field sources. Kim et al. (1991) considered a larger sample of 161 sources and found that those sources projected within one third of an Abell radius of the cluster center had a significant RM excess over sources with larger impact parameters. Kim et al. (1990) found that the RMs toward sources within 20′ of the Coma cluster center had an enhanced RM dispersion (by 38 ± 6 rad m^{-2}). From this excess they derived a magnetic field strength of 2.0 ± 1.1 μG assuming a cell size in the range 7–26 kpc. Feretti et al. (1995) found evidence from the RM distribution of the embedded cluster source NGC 4869 for smaller cell sizes ($\sim$1 kpc), and subsequently estimated the field strength in Coma to be 6.2 μG.

The most significant work in this area is the recent VLA survey by Clarke et al. (2001), in which they observed radio sources in and behind a representative sample of 16 Abell clusters at $z < 0.1$. They found enhanced rotation measures on the large majority of the lines of sight within 0.5 Mpc of the cluster centers (Figure 6), from which they derived an areal filling of the magnetic fields of 95%. Their modeling results in magnetic fields of $\sim$5 μG, assuming a cell size of 10 kpc. These clusters were chosen for their lack of cooling flows, but are otherwise unremarkable in their properties. With approximately one half their sources behind the clusters, these observations demonstrated an embedded powerful radio galaxy is not required to produce significant RMs. Another advantage of this technique is that it permits estimation of the spatial extent of the magnetic fields within the cluster ($\sim$0.5 Mpc). The areal filling factor of 95% (assuming constant magnetic fields in and among all clusters) suggests a relatively large volume-filling factor for the fields, with a formal (extreme) lower limit being about 8% for 10-kpc cell sizes.
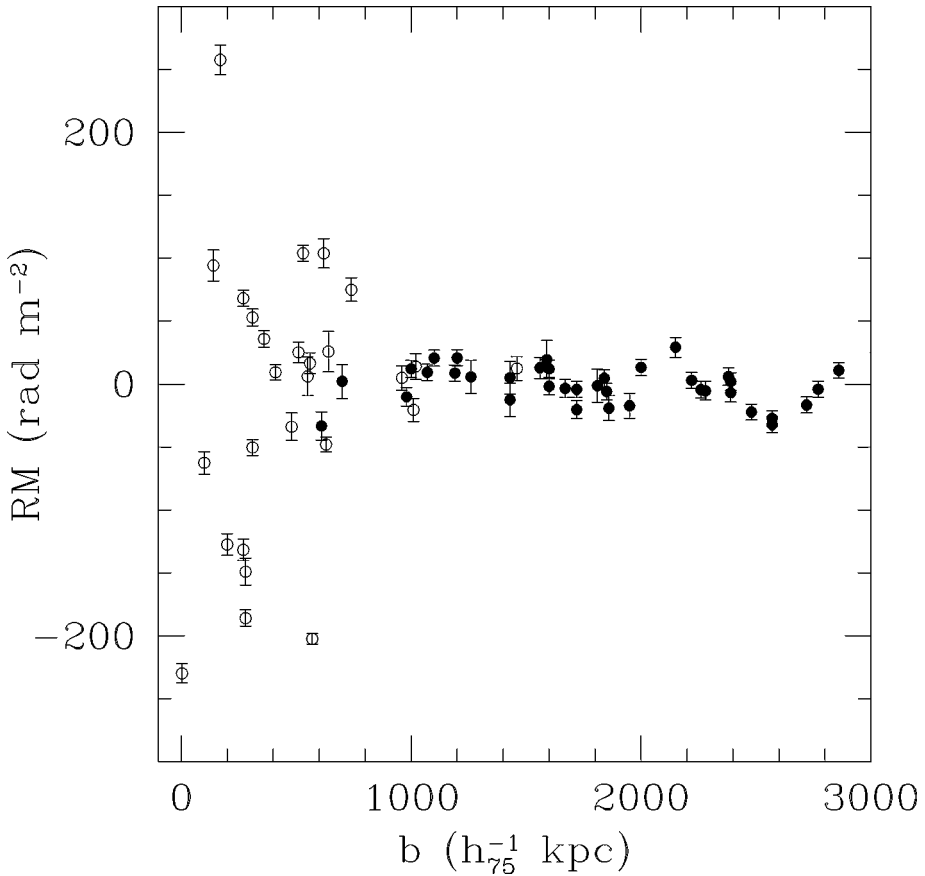
Figure 6   The integrated RM plotted as a function of source impact parameter in kiloparsecs for the sample of 16 Abell clusters described in Clarke et al. (2001). The *open symbols* represent sources viewed through the cluster, whereas the *closed symbols* represent the control sample of field sources.

High Redshift Sources

Radio galaxies and radio loud quasars have been detected to $z = 5.2$ (van Breugel 2000). The extended polarized emission from these sources provides an ideal probe of their environments through Faraday rotation observations. Extensive radio imaging surveys of $z > 2$ radio galaxies and quasars have shown large rotation measures, and Faraday depolarization, in at least 30% of the sources, indicating that the sources are situated behind dense Faraday screens of magnetized, ionized plasma (Chambers et al. 1990; Garrington et al. 1988; Carilli et al. 1994, 1997; Pentericci et al. 2000; Lonsdale et al. 1993; Athreya et al. 1998), with a

possible increase in this fraction with redshift (Pentericci et al. 2000). Drawing the analogy to lower z radio galaxies, these authors proposed that the high z sources may be embedded in magnetized (proto-) cluster atmospheres, with μG field strengths.

A difficulty with the study of high redshift sources is that the sources are typically small ($<$few arcseconds), requiring higher frequency observations (5 to 8 GHz) in order to properly resolve the source structure. This leads to two problems. First, the rest frame frequencies are then ≥ 20 GHz, such that only extreme values of Faraday rotation can be measured (RM ≥ 1000 rad m^{-2}). Second, only the flatter spectrum, higher surface brightness radio emitting structures in the sources are detected, thereby allowing for only a few lines-of-site through the ICM as RM probes. Imaging at frequencies of 1.4 GHz or lower with subarcsecond resolution is required to address this interesting issue.

INVERSE COMPTON X-RAY EMISSION

Cosmic magnetic fields can be derived by comparing inverse Compton X-ray emission and radio synchrotron radiation (Harris & Grindlay 1979, Rephaeli et al. 1987). Inverse Compton (IC) emission is the relativisitic extrapolation of the Sunyaev-Zel'dovich effect (Rephaeli 1995), involving up-scattering of the ambient photon field by the relativisitic particle population. The IC process involves two Lorentz transforms (to and from the rest frame of the electron), plus Thompson scattering in the rest frame of the electron, leading to $\nu_{IC} \sim \frac{4}{3}\gamma^2\nu_{bg}$, where ν_{IC} is the emergent frequency of the scattered radiation, γ is the electron Lorentz factor, and ν_{bg} is the incident photon frequency (Bagchi et al. 1998). From a quantum mechanical perspective, synchrotron radiation is directly analogous to IC emission, with synchrotron radiation being the up-scattering of the virtual photons that constitute the static magnetic field. Given a relativistic electron population, the IC emissivity is directly proportional to the energy density in the photon field, U_{bg}, whereas the synchrotron emissivity is proportional to the energy density in the magnetic field, U_B, leading to a simple proportionality between synchrotron and IC luminosity: $\frac{L_{syn}}{L_{IC}} \propto \frac{U_B}{U_{bg}}$. Given that they originate from the same (assumed power-law) relativistic electron population, IC X-rays and synchrotron radio emission share the same spectral index, α. The spectral index relates to the index for the power-law electron energy distribution, Γ, as $\Gamma = 2\alpha - 1$, and to the photon index as $\alpha - 1$.

In most astrophysical circumstances, U_{bg} is dominated by the cosmic microwave background (CMB), except in the immediate vicinity of active–star-forming regions and AGN (Brunetti et al. 2001a, Carilli et al. 2001). The Planck function at T = 2.73 K peaks near a frequency of $\nu_{bg} \sim 1.6 \times 10^{11}$ Hz, hence IC X-rays observed at 20 keV ($\nu_{IC} = 4.8 \times 10^{18}$ Hz), are emitted predominantly by electrons at $\gamma \sim 5000$, independent of redshift.[1] The corresponding radio synchrotron

---

[1] γ is independent of redshift because ν_{bg} increases as $1 + z$.

emission from $\gamma = 5000$ electrons peaks at a (rest frame) frequency of $\nu_{\mathrm{syn}} \sim 4.2 \,(\frac{B}{1\,\mu\mathrm{G}})\gamma^2$ Hz $= 100$ MHz (Bagchi et al. 1998).

Many authors have considered the problem of deriving magnetic fields by comparing synchrotron radio and inverse Compton X-ray emission (Blumenthal & Gould 1970, Harris & Grindlay 1979, Rephaeli et al. 1987, Feigelson et al. 1995, Bagchi et al. 1998). Assuming $\alpha = -1$, the magnetic field is given by:

$$B = 1.7(1 + z)^2 \left(\frac{S_{\mathrm{r}}\nu_{\mathrm{r}}}{S_{\mathrm{x}}\nu_{\mathrm{x}}}\right)^{0.5} \mu\mathrm{G}, \qquad (4)$$

where S_{r} and S_{x} are the radio and X-ray flux densities at observed frequencies ν_{r} and ν_{x}, respectively. Note that, unlike Faraday rotation measurements, the geometry of the field does not play a critical role in this calculation, except in the context of the electron pitch angle distribution (see "Reconciling IC- and RM-Derived Fields" below).

The principle difficulty in studying IC emission from clusters of galaxies is confusion by the thermal emission from the cluster atmosphere. One means of separating the two emission mechanisms is through spectroscopic X-ray observations at high energy. The IC emission will have a harder, power-law spectrum relative to thermal brehmstrahlung emission. Recent high-energy X-ray satellites such as Beppo/Sax and RXTE have revolutionized this field by allowing for sensitive observations to be made at energies well above 10 keV (Rephaeli 2002). Prior to these instruments, most studies of IC emission from clusters with radio halos only provided lower limits to the magnetic fields of about 0.1 μG (Rephaeli et al. 1987).

Recent observations of four clusters with radio halos with Beppo/Sax and RXTE have revealed hard X-ray tails that dominate the integrated emission above 20 keV (Rephaeli et al. 1999; Fusco-Femiano et al. 2001, 2000). In Figure 7, we reproduce the RXTE observations of the Coma cluster. The hard X-ray emission in these sources has a spectral index $\alpha = -1.3 \pm 0.3$, roughly consistent with the radio spectral index. Comparing the IC X-ray and radio synchrotron emission in these sources leads to a volume-averaged cluster magnetic field of 0.2 to 0.4 μG, with a relativistic electron energy density $\sim 10^{-13}$ erg cm^{-3}.

Spatially resolving X-ray observations can also be used to separate nonthermal and thermal X-ray emission in clusters. This technique has been used recently in the study of the steep spectrum radio relic source in Abell 85 (Bagchi et al. 1998). An X-ray excess relative to that expected for the cluster atmosphere is seen with the ROSAT PSPC detector at the position of the diffuse radio source in Abell 85 (see Figure 8). Bagchi et al. (1998) subtract a model of the thermal cluster X-ray emission in order to derive the IC contribution, from which they derive a magnetic field of 1.0 $\pm$ 0.1 μG.

Emission above that expected from the hot cluster atmosphere has also been detected in the extreme ultraviolet (EUV = 0.1 to 0.4 keV) in a few clusters (Berghöfer et al. 2000, Bowyer et al. 2001, Bonamente et al. 2001). It has been suggested that this emission may also be IC in origin, corresponding to relativistic electrons with $\gamma \sim 400$ (Atoyan & Völk 2000). However, the emission spectrum
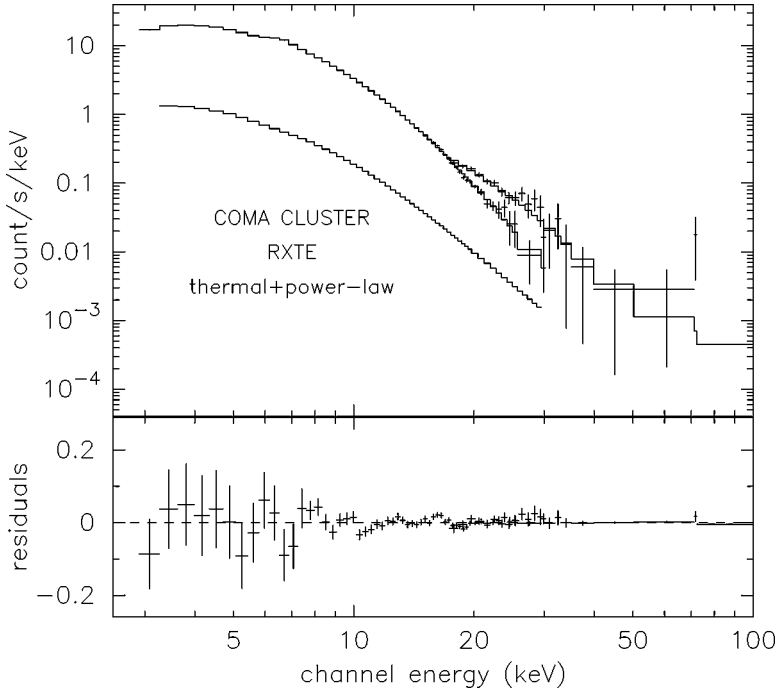
Figure 7 RXTE spectrum of the Coma cluster. Data and folded Raymond-Smith ($kT \simeq 7.51$ keV), and power-law (photon index $= 2.34$) models are shown in the *upper frame*; the latter component is also shown separately in the *lower line*. Residuals of the fit are shown in the *lower frame* (Rephaeli 2002).

is steep ($\alpha \leq -2$), and the EUV emitting regions are less extended than the radio regions. Neither of these properties are consistent with a simple extrapolation of the radio halo properties to low frequency (Bowyer et al. 2001). Also, the pressure in this low γ relativistic component would exceed that in the thermal gas by at least a factor of three (Bonamente et al. 2001).

Electron Lifetimes

An important point concerning IC and synchrotron emission from clusters is that of particle lifetimes. The lifetime of a relativistic electron is limited by IC losses off the microwave background to $t_{IC} = 7.7 \times 10^9 (\frac{300}{\gamma})(1 + z)^{-4}$ years (Sarazin 2002).[2] Relativistic electrons emitting in the hard X-ray band via IC scattering

---

[2]For $\gamma > 300$, IC losses dominate [or synchrotron losses for $B > 2.3 (1 + z)^2 \mu G$], whereas for lower γ electrons Brehmstrahlung losses dominate in cluster environments (Sarazin 2001b).
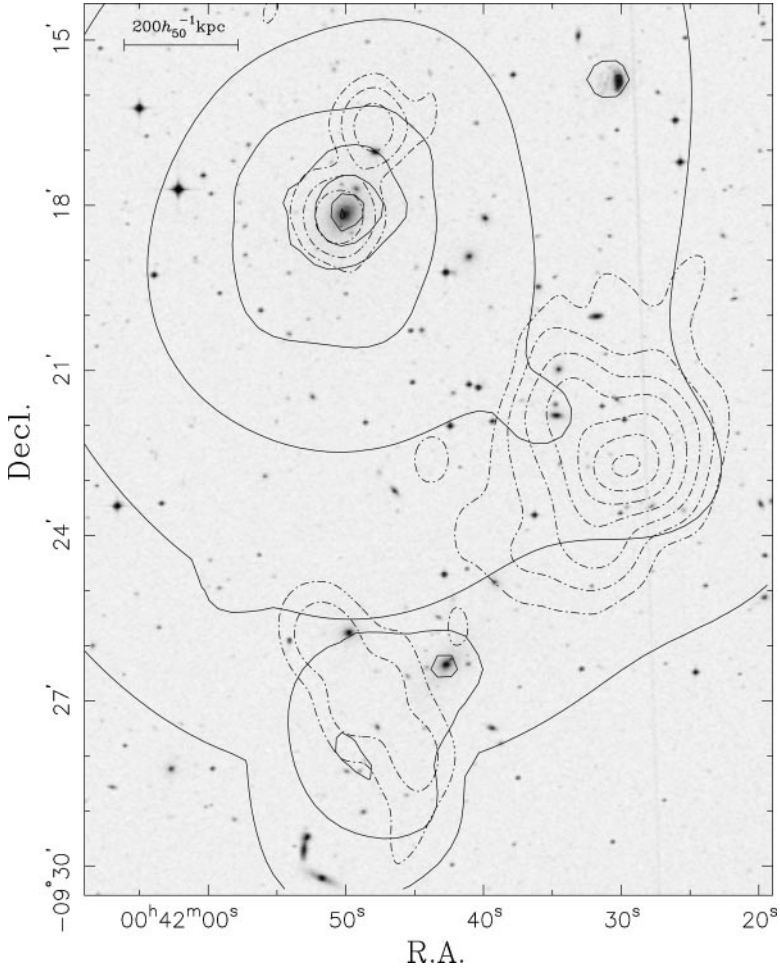
Figure 8 The cluster Abell 85 central region at different wavelengths. The photographic R-filter image (UK Schmidt Telescope and the Digitized Sky Survey) is shown in gray scale. Full contour lines show the multiscale wavelet reconstruction of the ROSAT PSPC X-ray data. The Ooty Synthesis Radio Telescope (OSRT) 326.5 MHz radio surface-brightness image is depicted using dot-dashed contour lines. All contours are spaced logarithmically (Bagchi et al. 1998).

of the CMB have lifetimes of about 10^9 years, whereas the lifetimes for 1.4 GHz synchrotron emitting electrons are a factor of four or so shorter in μG fields. Diffusion timescales (set by streaming along the tangled magnetic field) for cluster relativistic electrons are thought to be longer than the Hubble time (Sarazin 2002, Colafrancesco & Blasi 1998, Casse et al. 2001), making cluster atmospheres efficient traps of relativistic electrons, much like galaxy disks. The fact that the

diffusion timescales are much longer than the energy loss timescales for $\gamma > 10^4$ electrons requires in situ acceleration in order to explain radio halo sources (Schlikeiser et al. 1987).

Cluster merger shock fronts are obvious sites for first-order Fermi acceleration, whereas subsequent turbulence may lead to second-order (stochastic) Fermi acceleration (Brunetti et al. 2001b, Eilek 1999, Ensslin et al. 1998, Markevitch & Vikhlinin 2001). Active particle acceleration during cluster mergers provides a natural explanation for the observed correlation between cluster radio halos and substructure in cluster atmospheres (Govoni et al. 2001a), and between cluster radio luminosity and cluster atmosphere temperature, assuming that the gas temperature increases during a merger (Liang et al. 2000). Brunetti et al. (2001a) develop a two-phase model in which initial relativistic particle injection into the ICM occurs early in the cluster lifetime by starburst-driven winds from cluster galaxies, and/or by shocks in early subcluster mergers. The second phase involves re-acceleration of the radiatively aged particle population via more recent cluster mergers. Their detailed application of this model to the Coma cluster suggests a merger has occurred within the last 10^9 years.

Another mechanism proposed for in situ relativistic particle injection is secondary electron production via the decay of π-mesons generated in collisions between cosmic ray ions (mostly protons) and the thermal ICM (Dennison 1980, Dolag & Ensslin 2000). The important point, in this case, is that the energetic protons have radiative lifetimes orders of magnitude longer than the lower mass electrons. The problem with this hypothesis is that the predicted γ-ray fluxes exceed limits set by EGRET by a factor of 2 to 7 (Blasi & Colafrancesco 1999).

Reconciling IC- and RM-Derived Fields

The IC-estimated cluster magnetic fields are typically 0.2 to 1 μG, whereas those obtained using RM observations are a factor four to ten higher. Petrosian (2001) has considered this discrepancy in detail, and finds that the different magnetic field estimates can be reconciled in most cases by making a few reasonable assumptions concerning the electron energy spectrum and pitch-angle distribution.

First, an anisotropic pitch-angle distribution biased toward low angles would clearly weaken the radio synchrotron radiation relative to the IC X-ray emission. Such a distribution will occur naturally given that electrons at large pitch angles have greater synchrotron losses. A potential problem with this argument is that pitch-angle scattering of the relativistic electrons by Alfven waves self-induced by particles streaming along field lines is thought to be an efficient process in the ISM and ICM (Wentzel 1974), such that re-isotropization of the particle distribution will occur on a timescale short compared to radiative timescales. Petrosian (2001) points out that most derivations of magnetic fields from IC emission assume the electrons are gyrating perpendicular to the magnetic field lines. Just assuming an isotropic relativistic electron pitch-angle distribution raises the IC-estimated magnetic field by a factor of two or so.

Second, the IC hard X-ray emission is from relativistic electrons with $\gamma \sim 5000$. This corresponds to radio continuum emission at 100 MHz for μG magnetic fields. Most surveys of cluster radio halos have been done at 1.4 GHz (Giovanni et al. 1999, Govoni et al. 2001a), corresponding to electron Lorentz factors of $\gamma \sim 18000$. A steepening in the electron energy spectrum at Lorentz factors around 10^4 will reduce the 1.4 GHz radio luminosities, but retain the IC hard X-ray emission. For example, Petrosian (2001) finds that a change in the power-law index for the particle energy distribution from $\Gamma = -3$ to $\Gamma = -5$ (corresponding to $\alpha = -1$ to -2) at $\gamma \sim 10^4$ raises the IC-estimated fields to ~ 1 μG. Such a steepening of the electron energy spectrum at $\gamma \sim 10^4$ will arise naturally if no relativistic particle injection occurs over a timescale $\sim 10^8$ years (see "Electron Lifetimes" above). The problem in this case is the fine tuning required to achieve the break in the relevant energy range for a number of clusters. In general, a negatively curved (in log-space) electron energy distribution will inevitably lead to IC-estimated fields being lower than those estimated from 1.4 GHz radio observations, unless a correction is made for the spectral curvature.

Others have pointed out that magnetic substructure, or filamentation, can lead to a significant difference between fields estimated using the different techniques. A large relativistic electron population can be hidden from radio observations by putting them in weak-field regions (Feretti et al. 2001, Rephaeli et al. 1987, Rephaeli 2002, Goldshmidt & Rephaeli 1993, Rudnick 2000). A simple example of this is if the relativistic particles have a larger radial scale-length than the magnetic fields in the cluster. In this case, most of the IC emission will come from the weak-field regions in the outer parts of the cluster, whereas most of the Faraday rotation and synchrotron emission occurs in the strong-field regions in the inner parts of the cluster.

Another explanation for the discrepancy between IC- and RM-derived magnetic fields is to assume that the hard X-rays are not IC in origin, in which case the IC estimates become lower limits. A number of authors have considered high energy X-ray emission by nonthermal Brehmstrahlung, i.e., Brehmstrahlung radiation from a suprathermal tail of electrons arising via stochastic acceleration in a turbulent medium (Fermi II acceleration) (Blasi 2000, Sarazin 2002, Ensslin et al. 1999, Dogiel 2000). The problem with this hypothesis is the energetics: Brehmstrahlung is an inefficient radiation mechanism, with most of the collisional energy going into heat. Assuming an energy source is available to maintain the suprathermal tail, Petrosian (2001) shows that the collisional energy input by the suprathermal particles would be adequate to evaporate the cluster atmosphere on a timescale of $\leq 10^9$ years. Hence the mechanism maintaining the suprathermal tail must be short lived (Blasi 2000).

The current hard X-ray spectroscopic observations are limited to very low spatial resolution ($\sim 1°$), whereas X-ray imaging instruments have high energy cut-offs at around 10 keV. Likewise, sensitive arcminute resolution radio images for a large number of clusters are available only at 1.4 GHz, corresponding to electrons with Lorentz factors 3 to 4 times higher than those emitting hard X-rays. Both of these

limitations will be overcome in the coming years with the launch of hard-X-ray imaging satellites such as Constellation-X, and improvements in radio imaging capabilities at 300 MHz and below at the Very Large Array and the Giant Meter wave Radio Telescope.

COLD FRONTS

In order to maintain temperature gradients in X-ray clusters, the thermal conduction must be suppressed by two orders of magnitude relative to the classical Spitzer value (Mckee & Begelman 1990, Fabian 1994, Spitzer 1962). If not, cooler structures on scales of ~0.1 Mpc will be evaporated by thermal conduction from the hot surrounding medium on timescales of ~10^7 years. Examples of such cooler structures in clusters include cooling-flow cluster cores and X-ray corona surrounding large galaxies (Fabian 1994, Vikhlinin et al. 2001a), with temperature differences ranging from a factor of 2 to 5 relative to the hot ICM.

Cowie & McKee (1977) show that the conductivity can be suppressed by almost an order of magnitude below the Spitzer value in cases where the Coulomb mean free path (mfp) is comparable to the scale of thermal gradients owing to the development of electrostatic fields. For large-scale structure in cluster atmospheres, this reduction is not adequate because the mfp $\sim 1.2 \times 10^{22} (\frac{T}{5 \times 10^7 \, K})^2 (\frac{n}{0.001 \, cm^{-3}})^{-1}$ cm, or just a few kpc for a typical cluster.

The presence of magnetic fields will reduce the conductivity in a thermal plasma (Field 1965, Parker 1979, Binney & Cowie 1981, Chandran et al. 1999). The simple point is that the gyro radius for thermal electrons in the ICM is $\sim 2 \times 10^8$ $(\frac{B^{-1}}{1 \mu G})(\frac{T}{5 \times 10^7 \, K})$ cm, many orders of magnitude below the collisional mfp. Tribble (1993) shows that the presence of a cluster magnetic field will lead naturally to the development of a multiphase ICM, with thermally isolated regions on scales set by the magnetic structures [but compare Rosner & Tucker 1989).

The idea of magnetic suppression of thermal conductivity in cluster gas has been verified with the recent discovery of cold fronts in clusters of galaxies (Markevitch et al. 2000; Vikhlinin et al. 2001a,b). These fronts manifest themselves as sharp discontinuities in X-ray surface brightness (Figure 9). They are not shocks, because the increase in density is accompanied by a decrease in temperature such that there is no dramatic change in the pressure and entropy across the front (Markevitch et al. 2000, Ettori & Fabian 2000). These structures are interpreted as resulting from cluster mergers, where a cooler subcluster core falls into a hot ICM at sub- or trans-sonic velocities ($\sim 10^3$ km s^{-1}). A discontinuity is formed where the internal pressure of the core equals the combined ram and thermal pressure of the external medium. Gas beyond this radius is stripped from the merging subcluster, and the core is not penetrated by shocks owing to its high internal pressure.

The best example of a cluster cold front is that seen in Abell 3667 (see Figure 9) (Vikhlinin et al. 2001a,b). In this case, the temperature discontinuity occurs over

a scale of ~5 kpc, comparable to the collisional mfp, thereby requiring thermal isolation. Magnetic fields play a fundamental role in allowing for such structures in two ways: (*a*) by suppressing thermal conduction and (*b*) by suppressing Kelvin-Helmholtz mixing along the contact discontinuity. Vikhlinin et al. (2001a) present a model in which the field is tangentially sheared by fluid motions along the contact discontinuity. They invoke magnetic tension to suppress mixing, and show that the required magnetic pressure is between 10% and 20% of the thermal pressure. The implied fields are between 7 and 16 μG. They also argue that the fields cannot be much stronger than this, because dynamically dominant fields would suppress mixing along the entire front, which does not appear to be the case.

The existence of cold fronts provides strong evidence for cluster magnetic fields. However, the field strengths derived correspond to those in the tangentially sheared boundary region around the front. Relating these back to the unperturbed cluster field probably requires a factor of a few reduction in field strength, implying unperturbed field strengths between 1 and 10 μG, although the exact scale factor remains uncertain (Vikhlinin et al. 2001b).

MAGNETIC SUPPORT OF CLUSTER GAS AND THE BARYON CRISIS

Two interesting issues have arisen in the study of cluster gas and gravitational masses. First is the fact that total gravitating masses derived from weak gravitational lensing are a factor of a few higher than those derived from X-ray observations of cluster atmospheres, assuming hydrostatic equilibrium of isothermal atmospheres (Loeb & Mao 1994, Miralda-Escude & Babul 1995). Second is the baryon crisis, in which the baryonic mass of a cluster, which is dominated by the mass of gas in the hot cluster atmosphere, corresponds to roughly 5% of the gravitational mass derived assuming hydrostatic equilibrium for an isothermal cluster atmosphere. This baryon fraction is a factor of three to five larger than the baryon fraction dictated by big bang nucleosynthesis in inflationary world models (White et al. 1993).

A possible solution to both these problems is to invoke nonthermal pressure support for the cluster atmosphere, thereby allowing for larger gravitating masses relative to those derived assuming hydrostatic equilibrium. A number of authors have investigated the possibility of magnetic pressure support for cluster atmospheres (Loeb & Mao 1994, Miralda-Escude & Babul 1995, Dolag & Schindler 2000). The required fields are about 50 μG, which is an order of magnitude, or more, larger than the measured fields in most cases, except perhaps in the inner 10s of kpc of cooling-flow clusters. For most relaxed clusters, Dolag & Schindler (2000) find that magnetic pressure affects hydrostatic mass estimates by at most 15%.

Other mechanisms for nonthermal pressure support of cluster atmospheres involve motions of the cluster gas other than thermal, such as turbulent or bulk

motions owing to a recent cluster merger (Mazzotta et al. 2001, Wu 2000). For relaxed clusters, a number of groups have shown that the lensing and X-ray mass estimates can be reconciled by using nonisothermal models for the cluster atmospheres, i.e., by allowing for radial temperature gradients (Allen et al. 2001b, Markevitch et al. 1999).

GZK LIMIT

Greisen (1966) and Zatsepin & Kuzmin (1966) pointed out that cosmic rays with energies $>10^{19}$ eV lose energy due to photo-pion production through interaction with the CMB. These losses limit the propagation distance for 10^{20} eV particles to about 60 Mpc. Yet, no clear correlation has been found between the arrival direction of high energy cosmic rays and the most likely sites of origin for EeV particles, namely, AGN at distances less than 60 Mpc (Elbert & Sommers 1995, Biermann 1999). One possible solution to the GZK paradox is to assume the energetic particles are isotropized in the IGM by tangled magnetic fields, effectively randomizing their observed arrival direction. Such isotropization requires fields in the local super-cluster ≥ 0.3 μG (Farrar & Piran 2000; but compare Isola et al. 2000).

SYNTHESIS

In Table 1, we summarize the cluster magnetic field measurements. Given the limitations of the current instrumentation, the limited number of sources studied thus far, and the myriad physical assumptions involved with each method, we are encouraged by the order-of-magnitude agreement between cluster field strengths derived from these different methods. Overall, the data are consistent with cluster atmospheres containing $\sim \mu$G fields, with perhaps an order-of-magnitude scatter in field strength between clusters, or within a given cluster.

TABLE 1 Cluster magnetic fields

Method	Strength μG	Model parameters
Synchrotron halos	0.4–1	Minimum energy, $k = \eta = 1$, $\nu_{low} = 10$ MHz, $\nu_{high} = 10$ GHz
Faraday rotation (embedded)	3–40	Cell size $= 10$ kpc
Faraday rotation (background)	1–10	Cell size $= 10$ kpc
Inverse Compton	0.2–1	$\alpha = -1$, $\gamma_{radio} \sim 18000$, $\gamma_{xray} \sim 5000$
Cold fronts	1–10	Amplification factor ~ 3
GZK	>0.3	AGN $=$ site of origin for EeV CRs

The RM observations of embedded and background radio sources suggest that μG magnetic fields with high areal filling factors are a standard feature in clusters, and that the fields extend to large radii (0.5 Mpc or more). The RM observations of extended radio galaxies embedded in clusters impose order on the fields, with coherence scales of order 10 kpc, although larger scale coherence in overall RM sign can be seen in some sources. Observations of inverse Compton emission from a few clusters with radio halos provide evidence against much stronger, pervasive, and highly tangled fields.

In most clusters the fields are not dynamically important, with magnetic pressures one to two orders of magnitude below thermal gas pressures. But the fields play a fundamental role in the energy budget of the ICM through their effect on heat conduction, as is dramatically evident in high-resolution X-ray observations of cluster cold fronts.

If most clusters contain μG magnetic fields, then why don't most clusters have radio halos? The answer may be the short lifetimes of the relativistic electrons responsible for the synchrotron radio emission (see "Electron Lifetimes" above). Without re-acceleration or injection of relativistic electrons, a synchrotron halo emitting at 1.4 GHz will fade in about 10^8 years due to synchrotron and inverse Compton losses. This may explain the correlation between radio halos and cluster mergers, and the anticorrelation between radio halos and clusters with relaxed X-ray morphologies. In this case, the fraction of clusters with radio halos should increase with decreasing survey frequency.

The existence of μG-level fields in cluster atmospheres appears well established. The challenge for observers now becomes one of determining the detailed properties of the fields, and how they relate to other cluster properties. Are the fields filamentary, and to what extent do the thermal and nonthermal plasma mix in cluster atmospheres? What is the radial dependence of the field strength? How do the fields depend on cluster atmospheric parameters, such as gas temperature, metalicity, mass, substructure, or density profile? How do the fields evolve with cosmic time? And do the fields extend to even larger radii, perhaps filling the IGM? The challenge to the theorists is simpler: How were these fields generated? This topic is considered briefly in the next section.

FIELD ORIGIN

When attempting to understand the behavior of cosmic magnetic fields, a critical characteristic to keep in mind is their longevity. The Spitzer conductivity (Spitzer 1962) of the ICM is $\sigma \sim 3 \times 10^{18}$ sec^{-1} (for comparison, the conductivity of liquid mercury at room temperature is 10^{16} sec^{-1}). The timescale for magnetic diffusion in the ICM is then $\tau_{\text{diff}} = 4\pi\sigma(\frac{L}{c})^2 \sim 10^{36}(\frac{L}{10\,\text{kpc}})^2$ years, where L is the spatial scale for magnetic fluctuations. The magnetic Reynold's number is $R_m = \frac{\tau_{\text{diff}}}{\tau_{\text{conv}}} \sim 10^{29}(\frac{L}{10\,\text{kpc}})(\frac{V}{1000\,\text{km s}^{-1}})$, where $\tau_{\text{conv}} = $ the convective timescale $= \frac{L}{V}$, and V is the bulk fluid velocity. The essentially infinite diffusion timescale for the

fields implies that once a field is generated within the ICM, it will remain extant unless some anomalous resistive process occurs, e.g., reconnection via plasma-wave generation in shocks.

Perhaps the simplest origin for cluster magnetic fields is compression of an intergalactic field. Clusters have present-day overdensities $\delta \sim 10^3$. In order to get $B_{ICM} > 10^{-7}$ G by adiabatic compression ($B \propto \delta^{\frac{2}{3}}$) then requires IGM fields $B_{IGM} > 10^{-9} \, \mu$G.

Of course, this solution merely pushes the field origin problem from the ICM into the IGM. An upper limit to IGM fields of 10^{-9} G is set by Faraday rotation measurements of high z radio loud QSOs, assuming a cell size of order 1 Mpc (Kronberg 1996, Blasi et al. 1999). A limit to IGM magnetic fields at the time of recombination can also be set by considering their affect on the CMB. Dynamically significant magnetic fields will exert an anisotropic pressure on the gas, which must be balanced by gravity. Detailed studies of this phenomenon in the context of recent measurements of the CMB anisotropies shows that the comoving IGM fields[3] must be less than a few $\times \, 10^{-9}$ G (Barrow et al. 1997, Barrow & Subramanian 1998, Clarkson & Coley 2001, Adams et al. 1996). A comoving field of 10^{-9} G at recombination would lead to Faraday rotation of the polarized CMB emission by $1°$ at an observing frequency of 30 GHz, a measurement that is within reach of future instrumentation (Kosowsky & Loeb 1996, Grasso & Rubinstein 2001). Considerations of primordial nucleosynthesis and the affect of magnetic fields on weak interactions and electron densities imply upper limits to comoving IGM fields of 10^{-7} G (Grasso & Rubinstein 1995).

The origin of IGM magnetic fields has been considered by many authors. One class of models involves large-scale field generation prior to recombination. An excellent review of pre-recombination magnetic field generation is presented by Grasso & Rubinstein (2001). Early models for pre-recombination field generation involved the hydrodynamical Biermann battery effect (Biermann 1950). In general, the hydrodynamic battery involves charge separation arising from the fact that electrons and protons have the same charge, but very different masses. For instance, protons will have larger Coulomb stopping distances than electrons, and be less affected by photon drag. Harrison (1970) suggested that photon drag on protons relative to electrons in vortical turbulence during the radiation era could lead to charge separation, and hence, magnetic field generation by electric currents. Subsequent authors have argued strongly against vortical density perturbations just prior to recombination, because vortical (and higher order) density perturbations decay rapidly with the expansion of the universe (Rees 1987). This idea has been revisited recently in the context of vortical turbulence generated by moving cosmic strings (Vachaspati & Vilenkin 1991, Avelino & Shellard 1995). Other mechanisms for field generation prior to recombination include battery affects during the quark-hadron (QCD) phase transition (Quashnock et al. 1989), dynamo

---

[3]Comoving fields correspond to equivalent present-epoch field strengths, i.e., corrected for cosmic expansion assuming flux freezing.

mechanisms during the electro-weak (QED) phase transition (Baym et al. 1996), and mechanisms relating to the basic physics of inflation (Turner & Widrow 1988).

A problem with all these mechanisms is the survivability of the fields on relevant scales during the radiation era. Battaner & Lesch (2000) argue that magnetic and photon diffusion will destroy fields on comoving scales $\leq$ few Mpc during this epoch, thereby requiring generation of the fields in the post-recombination universe by normal plasma processes during proto-galactic evolution (see also Lesch & Birk 1998).

Models for post-recombination IGM magnetic field generation typically involve ejection of the fields from normal or active galaxies (Kronberg 1996). A simple but cogent argument for this case is that the metalicity of the ICM is typically about 30% solar, implying that cluster atmospheres have been polluted by outflows from galaxies (Aguirre et al. 2001). A natural extension of this idea would be to include magnetic fields in the outflows (Goldshmidt & Rephaeli 1993). It has also been suggested that IGM fields could be generated through turbulent dynamo processes and/or shocks occurring during structure formation (Zweibel 1988, Kulsrud et al. 1997, Waxman & Loeb 2000), or by battery effects during the epoch of reionization (Gnedin et al. 2000).

Seed magnetic fields will arise in the earliest stars via the normal gas kinematical Biermann battery mechanism. These fields are amplified by the $\alpha - \Omega$ dynamo operating in convective stellar atmospheres (Parker 1979), and then are ejected into the ISM by stellar outflows and supernova explosions. The ISM fields can then be injected into the IGM by winds from active star-forming galaxies (Heckman 2001). Kronberg et al. (1999) consider this problem in detail and show that a population of dwarf starburst galaxies at $z \geq 6$ could magnetize almost 50% of the universe, but that at lower redshifts the IGM volume is too large for galaxy outflows to affect a significant fraction of the volume.

De Young (1992) and Rephaeli (1988) show that galaxy outflows, and/or gas stripping by the ICM, in present-day clusters are insufficient to be solely responsible for cluster fields ~ 1 μG without invoking subsequent dynamo amplification of the field strength by about an order of magnitude in the cluster atmosphere. A simple argument in this case is that the mean density ratio of the ICM versus the ISM, $\delta \sim 0.01$, such that ICM fields would be weaker than ISM fields by $\delta^{\frac{2}{3}} \sim 0.05$, corresponding to maximum ICM fields of 0.2 to 0.5 μG.

Fields can be ejected from Active Galactic Nuclei (AGN) by relativistic outflows (radio jets) and Broad Absorption Line outflows (BALs) (Rees & Setti 1968, Daly & Loeb 1990). The ultimate origin of the fields in this case may be a seed field generated by a gas kinematic battery operating in the dense accretion disk around the massive black hole, plus subsequent amplification by an $\alpha - \Omega$ dynamo in the rotating disk (Colgate & Li 2000). Detailed consideration of this problem (Furlanetto & Loeb 2001, Kronberg et al. 2001) using the statistics for high z QSO populations shows that by $z \sim 3$, between 5% and 20% of the IGM may be permeated by fields with energy densities corresponding to ≥ 10% the thermal energy density of the photoionized IGM at 10^4 K, corresponding to comoving field strengths of order 10^{-9} μG.

Kronberg et al. (2001) point out that powerful double radio sources such as Cygnus A (radio luminosities $\sim 10^{45}$ erg s^{-1}) typically have total magnetic energies of about 10% of that of the ICM as a whole. Hence, about ten powerful double radio sources over a cluster lifetime would be adequate to magnetize the cluster at the μG level.

Galaxy turbulent wakes have been proposed as a means of amplifying cluster magnetic fields (Jaffe 1980, Tribble 1993, Ruzmaikin et al. 1989). The problem in this case is that the energy appears to be insufficient, with expected field strengths of at most ~ 0.1 μG. Also, the size scale of the dominant magnetic structures is predicted to be significantly smaller than the 5 to 10 kpc scale sizes observed (Goldshmidt & Rephaeli 1993, De Young 1992).

Cluster mergers are the most energetic events in the universe since the big bang, releasing of order 10^{64} ergs in gravitational binding energy (Sarazin 2002). For comparison, the total thermal energy in the cluster atmosphere is $\sim 10^{63}$ $(\frac{M_{gas}}{10^{14} M_\odot})(\frac{T}{5 \times 10^7 K})$ ergs, and the total energy contained in the cluster magnetic fields is $\sim 10^{60}(\frac{B}{1 \mu G})^2$ ergs. Hence, only a fraction of a percent of the cluster merger energy need be converted into magnetic fields. One possibility for merger-generated magnetic fields is a rotational dynamo associated with helical turbulence driven by off-center cluster mergers. This mechanism requires net cluster rotation—a phenomenon that has yet to be seen in cluster galaxy velocity fields (compare Dupke & Bregman 2001). The lack of observed rotation for clusters suggests low-impact parameters for mergers (≤ 100 kpc) on average (Sarazin 2002), as might arise if most mergers occur along filamentary large-scale structure (Evrard & Gioia 2002). The energetics of even slightly off-center cluster mergers is adequate to generate magnetic fields at the level observed, but the slow cluster rotation velocities (≤ 100 km s^{-1}) imply only one or two rotations in a Hubble time (Colgate & Li 2000), which is insufficient for mean field generation via the inverse cascade of the $\alpha - \Omega$ dynamo (Parker 1979).

A general treatment of the problem of magnetic field evolution during cluster formation comes from numerical studies of heirarchical merging of large-scale structure including an initial intergalactic field $\sim 10^{-9}$ G (Dolag & Schindler 2000, Roettiger et al. 1999). These studies show that a combination of adiabatic compression and nonlinear amplification in shocks during cluster mergers may lead to ICM mean fields of order 1 μG.

A related phenomenon is field amplification by (possible) cooling flows. Soker & Sarazin (1990) have considered this mechanism in detail, and show that the amplification could be a factor of 10 or larger in the inner 10s of kpc. They predict a strong increase in RMs with radius ($\propto r^2$), with centrally peaked radio halos. Such an increase may explain the extreme RM values seen in powerful radio sources at the centers of cooling flow clusters (see "Cluster Center Sources" above), although the existence of gas inflow in these systems remains a topic of debate (Binney 2002).

Overall, there are a number of plausible methods for generating cluster magnetic fields, ranging from injection of fields into the IGM (or early ICM) by active star-forming galaxies and/or radio jets at high redshift, to field amplification by cluster

mergers. It is likely that a combination of these phenomena give rise to the μG fields observed in nearby cluster atmospheres. Tests of these mechanisms will require observations of (proto-) cluster atmospheres at high redshift, and a better understanding of the general IGM field.

ACKNOWLEDGMENTS

The *Annual Review of Astronomy and Astrophysics* is online at
http://astro.annualreviews.org

LITERATURE CITED

Adams J, Danielsson UH, Grasso D, Rubinstein H. 1996. *Phys. Rev. D* 388:253–58

Aguirre A, Hernquist L, Schaye J, Katz N, Weinberg D, Gardner J. 2001. *Ap. J.* 561:521–49

Alexander P, Brown MT, Scott PF. 1984. *MNRAS* 209:851–68

Allen SW, Ettori S, Fabian AC. 2001b. *MNRAS* 324:877–90

Allen SW, Taylor GB, Nulsen PEJ, Johnstone RM, David LP, et al. 2001a. *MNRAS* 324:842–58

Athreya RM, Kapahi VK, McCarthy PJ, van Breugel W. 1998. *Astron. Astrophys.* 329:809–20

Atoyan AM, Völk HJ. 2000. *Ap. J.* 535:45–52

Avelino PP, Shellard EPS. 1995. *Phys. Rev. D* 51:5946–49

Bagchi J, Pislar V, Neto GBL. 1998. *MNRAS* 296:L23–28

Barrow JD, Ferreira PG, Silk J. 1997. *Phys. Rev. Lett.* 78:3610–13

Barrow JD, Subramanian K. 1998. *Phys. Rev. Lett.* 81:3575–79

Battaner E, Lesch H. 2000. *An. Fis.* In press astro-ph/0003370

Baym G, Bödeker D, McLerran L. 1996. *Phys. Rev. D* 53:662–67

Beck R, Brandenburg A, Moss D, Shukurov A, Sokoloff D. 1996. *Annu. Rev. Astron. Astrophys.* 34:155–206

Begelman MC, Blandford RD, Rees MJ. 1984. *Rev. Mod. Phys.* 56:255–351

Berghöfer TW, Bowyer S, Korpela E. 2000. *Ap. J.* 545:695–700

Bicknell GV, Cameron RA, Gingold RA. 1990. *Ap. J.* 357:373–87

Biermann L. 1950. *Z. Naturforsch. Tiel A* 5:65

Biermann PL. 1999. *Astrophys. Space Sci.* 264:423–35

Binney J. 2002. In *Particles and Fields in Radio Galaxies*, ed. RA Laing, KM Blundell. San Francisco: Astron. Soc. Pac. In press

Binney J, Cowie LL. 1981. *Ap. J.* 247:464–72

Blasi P. 2000. *Ap. J. Lett.* 532:L9–12

Blasi P, Burles S, Olinto AV. 1999. *Ap. J. Lett.* 514:L79–82

Blasi P, Colafrancesco S. 1999. *Astropart. Phys.* 12:169–83

Blumenthal GR, Gould RJ. 1970. *Rev. Mod. Phys.* 42:237–70

Böhringer H, Feretti L, Schuecker P, eds. 1999. *Diffuse Thermal and Relativistic Plasma in Galaxy Clusters*. MPE Rep. 271

Bonamente M, Lieu R, Nevalainen J, Kaastra JS. 2001. *Ap. J. Lett.* In press

Bowyer S, Korpela E, Berghöfer T. 2001. *Ap. J. Lett.* 548:L135–38

Bridle AH, Perley RA. 1984. *Annu. Rev. Astron. Astrophys.* 22:319–58

Brunetti G, Setti G, Feretti L, Giovannini G. 2001a. *MNRAS* 320:365–78

Brunetti G, Setti G, Feretti L, Giovannini G. 2001b. *New Astron.* 6:1–15

Buote D. 2001. *Ap. J.* 553:L15–18

Burbidge GR. 1959. *Ap. J.* 129:849–51

Burn BJ. 1966. *MNRAS* 133:67–83

Carilli CL, et al. 1997. In *Extragalactic Radio Sources*, ed. C Fanti, R Ekers, p. 159. Dordrecht: Kluwer

Carilli CL, et al. 2001. In *Starburst Galaxies Near and Far*, ed. L Tacconi, D Lutz, pp. 309–17. Berlin: Springer-Verlag. In press

Carilli CL, Owen FN, Harris DE. 1994. *Astron. J.* 107:480–93

Carilli CL, Perley RA, Dreher JW. 1988. *Ap. J.* 334:L73–76

Carilli CL, Roettgering HJA, van Ojik R, Miley GK, van Breugel WJM. 1997. *Astrophys. J. Suppl. Ser.* 109:1

Casse F, Lemoine M, Pelletier G. 2001. *Phys. Rev. D.* 65:3002–17

Cavaliere A, Fusco-Femiano R. 1976. *Astron. Astrophys.* 49:137–44

Chambers KC, Miley GK, van Breugel WJM. 1990. *Ap. J.* 363:21–39

Chandran BDG, Cowley SC, Albright B. 1999. See Böhringer et al. 1999, pp. 242–46

Clarke TE, Kronberg PP, Böhringer H. 2001. *Ap. J.* 547:L111–14

Clarkson CA, Coley AA. 2001. *Class. Quantum Gravity* 18:1305–10

Colafrancesco S, Blasi P. 1998. *Astropart. Phys.* 9:227–46

Colgate SA, Li H. 2000. In *Highly Energetic Physical Processes and Mechanisms for Emission from Astrophysical Plasmas. Proc. IAU Symp. 195, San Francisco*, pp. 255–65. San Francisco: Astron. Soc. Pac.

Condon JJ, Cotton WD, Greisen EW, Yin QF, Perley RA, et al. 1998. *Astron. J.* 115:1693–716

Cowie LL, McKee CF. 1977. *Ap. J.* 211:135–46

Daly RA, Loeb A. 1990. *Ap. J.* 364:451–55

Dennison B. 1980. *Ap. J.* 239:L93–96

De Young DS. 1992. *Ap. J.* 386:464–72

Dogiel VA. 2000. *Astron. Astrophys.* 357:66–74

Dolag K, Ensslin TA. 2000. *Astron. Astrophys.* 362:151–57

Dolag K, Schindler S. 2000. *Astron. Astrophys.* 364:491–96

Dolag K, Schindler S, Govoni F, Feretti L. 2001. *Astron. Astrophys.* 378:777–86

Dreher JW, Carilli CL, Perley RA. 1987. *Ap. J.* 315:611–25

Dupke RA, Bregman JN. 2001. *Ap. J.* 547:705–13

Eilek JA. 1999. See Böhringer et al. 1999, pp. 71–76

Eilek JA, Owen FN. 2002. *Ap. J.* In press

Elbert JW, Sommers P. 1995. *Ap. J.* 441:151–61

Ensslin TA, Biermann PL, Klein U, Kohle S. 1998. *Astron. Astrophys.* 332:395–409

Ensslin TA, Gopal-Krishna XX. 2001. *Astron. Astrophys.* 366:26–34

Ensslin TA, Lieu R, Biermann PL. 1999. *Astron. Astrophys.* 344:409–20

Ettori S, Fabian AC. 2000. *MNRAS* 317:L57–59

Evrard AE, Gioia IM. 2002. In *Merging Processes in Clusters of Galaxies*, ed. L Feretti, IM Gioia, G Giovannini. Dordrecht: Kluwer. In press

Fabbiano G, Schwartz DA, Schwarz J, Doxsey RE, Johnston M. 1979. *Ap. J.* 230:L67–71

Fabian AC. 1994. *Annu. Rev. Astron. Astrophys.* 32:277–318

Fabian AC, Nulsen PEJ, Canizares CR. 1991. *Astron. Astrophys. Rev.* 2:191–226

Fanaroff BL, Riley JM. 1974. *MNRAS* 167: L31–35

Farrar GR, Piran T. 2000. *Phys. Rev. Lett.* 84:3527–30

Feigelson ED, Laurent-Muehleisen SA, Kollgaard RI, Fomalont EB. 1995. *Ap. J. Lett.* 449:L149–52

Felten JB. 1996. In *Clusters, Lensing and the Future of the Universe*, ed. V Trimble, A Reisenegger, 88:271–73. San Francisco: Astron. Soc. Pac. Conf. Ser.

Feretti L. 1999. See Böhringer et al. 1999, pp. 3–8

Feretti L, Dallacasa D, Giovannini G, Tagliani A. 1995. *Astron. Astrophys.* 302:680–90

Feretti L, Dallacasa D, Govoni F, Giovannini G, Taylor GB, Klein U. 1999. *Astron. Astrophys.* 344:472–82

Feretti L, Fusco-Femiano R, Giovannini G, Govoni F. 2001. *Astron. Astrophys.* 373:106–12

Feretti L, Giovannini G. 1998. In *A New View of An Old Cluster: Untangling Coma Berenices*, ed. A Mazure, F Casoli, F Durret, D Gerbal, pp. 123. Singapore: World Sci.

Field GB. 1965. *Ap. J.* 142:531–67

Forman W, Kellogg E, Gursky H, Tananbaum H, Giacconi R. 1972. *Ap. J.* 178:309

Furlanetto S, Loeb A. 2001. *Ap. J.* 556:619–34

Fusco-Femiano R, Dal Fiume D, De Grandi S, Feretti L, Giovannini G, et al. 2000. *Ap. J. Lett.* 534:L7–10

Fusco-Femiano R, Dal Fiume D, Orlandini M, Brunetti G, Feretti L, Giovannini G. 2001. *Ap. J. Lett.* 552:L97–100

Garrington ST, Leahy JP, Conway RG, Laing RA. 1988. *Nature* 331:147–49

Ge JP, Owen FN. 1993. *Astron. J.* 105:778–87

Giovannini G, Feretti L. 2000. *New Astron.* 5:335–47

Giovannini G, Feretti L, Venturi T, Kim K-T, Kronberg PP. 1993. *Ap. J.* 406:399–406

Giovannini G, Tordi M, Feretti L. 1999. *New Astron.* 4:141–55

Gnedin NY, Ferrara A, Zweibel EG. 2000. *Ap. J.* 539:505–16

Goldshmidt O, Rephaeli Y. 1993. *Ap. J.* 411: 518–28

Govoni F, Feretti L, Giovannini G, Böhringer H, Reiprich TH, Murgia M. 2001a. *Astron. Astrophys.* 376:803–69

Govoni F, Taylor GB, Dallacasa D, Feretti L, Giovannini G. 2001b. *Astron. Astrophys.* 379:807–22

Grasso D, Rubinstein HR. 1995. *Nucl. Phys. B* 43:303–7

Grasso D, Rubinstein HR. 2001. *Phys. Rep.* 348:163–266

Greisen K. 1966. *Phys. Rev. Lett.* 16:748–58

Hanisch RJ. 1982. *Astron. Astrophys.* 116:137–46

Harris DE, Grindlay JE. 1979. *MNRAS* 188:25–37

Harris DE, Stern CP, Willis AG, Dewdney PE. 1993. *Astron. J.* 105:769–77

Harrison ER. 1970. *MNRAS* 147:279

Heckman TM. 2001. In *Extragalactic Gas at Low Redshift*, ed. J Mulchaey, J Stocke, San Francisco: Astron. Soc. Pac.

Hennessy GS, Owen FN, Eilek JA. 1989. *Ap. J.* 347:144–51

Isola C, Lemoine M, Sigl G. 2002. *Phys. Rev. D* 65:023004 astro-ph/0104289

Jaffe WJ. 1977. *Radio Astronomy and Cosmology. IAU Symp. 74*, pp. 305

Jaffe WJ. 1980. *Ap. J.* 241:925–27

Jones C, Mandel E, Schwarz J, Forman W, Murray SS, Harnden FR. 1979. *Ap. J. Lett.* 234:L21–24

Kempner JC, Sarazin CL. 2001. *Ap. J.* 548:639–51

Kim KT, Kronberg PP, Dewdney PE, Landecker TL. 1990. *Ap. J.* 355:29–37

Kim KT, Kronberg PP, Tribble PC. 1991. *Ap. J.* 379:80–88

Kosowsky A, Loeb A. 1996. *Ap. J.* 469:1–6

Kronberg PP. 1996. *Space Sci. Rev.* 75:387–99

Kronberg PP, Dufton QB, Li H, Colgate SA. 2001. *Ap. J.* 560:178–86

Kronberg PP, Lesch H, Hopp U. 1999. *Ap. J.* 511:56–64

Kulsrud RM. 1999. *Annu. Rev. Astron. Astrophys.* 37:37–64

Kulsrud RM, Cen R, Ostriker JP, Ryu D. 1997. *Ap. J.* 480:481–91

Large MI. 1959. *Nature* 183:1663–64

Lesch H, Birk GT. 1998. *Phys. Plasmas* 5: 2773–76

Liang H, Hunstead RW, Birkinshaw M, Andreani P. 2000. *Ap. J.* 544:686–701

Loeb A, Mao S. 1994. *Ap. J. Lett.* 435:L109–12

Lonsdale CJ, Barthel PD, Miley GK. 1993. *Astrophys. J. Suppl. Ser.* 87:63

Markevitch M, Ponman TJ, Nulsen PEJ, Bautz MW, Burke DJ, et al. 2000. *Ap. J.* 541:542–49

Markevitch M, Vikhlinin A. 2001. *Ap. J.* 563: 95–102

Markevitch M, Vikhlinin A, Forman WR, Sarazin CL. 1999. *Ap. J.* 527:545–53

Mazzotta P, Markevitch M, Vikhlinin A, Forman WR, David LP, VanSpeybroeck L. 2001. *Ap. J.* 555:205–14

McKee CF, Begelman MC. 1990. *Ap. J.* 358: 392–98

Meyer P. 1969. *Annu. Rev. Astron. Astrophys.* 7:1–38

Miley G. 1980. *Annu. Rev. Astron. Astrophys.* 18:165–218

Miralda-Escude J, Babul A. 1995. *Ap. J.* 449: 18–27

Mitton S. 1971. *MNRAS* 153:133–43

Owen F, Morrison G, Vogues W. 1999. Radio halos in luminous RASS clusters. See Böhringer, et al. 1999, pp. 9–11

Pacholczyk AG. 1970. *Radio Astrophysics.* San Francisco: Freeman

Parker EN. 1979. *Cosmical Magnetic Fields, Their Origin and Their Activity.* Oxford: Clarendon

Pentericci L, Van Reeven W, Carilli CL, Röttgering HJA, Miley GK. 2000. *Astron. Astrophys. Suppl. Ser.* 145:121–59

Perley RA, Taylor GB. 1991. *Astron. J.* 101:1623–31

Petrosian V. 2001. *Ap. J.* 557:560–72

Quashnock JM, Loeb A, Spergel DN. 1989. *Ap. J. Lett.* 344:L49–51

Rees MJ. 1987. *Q. J. R. Astron. Soc.* 28:197–206

Rees MJ, Setti G. 1968. *Nature* 219:127–31

Rephaeli Y. 1988. *Comm. Mod. Phys.* 12:265–79

Rephaeli Y. 1995. *Annu. Rev. Astron. Astrophys.* 33:541–80

Rephaeli Y. 2001. In *High Energy Gamma-Ray Astronomy.* In press astro-ph/0101363

Rephaeli Y, Gruber DE, Blanco P. 1999 *Ap. J. Lett.* 511:L21–24

Rephaeli Y, Gruber DE, Rothschild RE. 1987. *Ap. J.* 320:139–44

Roettiger K, Stone JM, Burns JO. 1999. *Ap. J.* 518:594–602

Rosner R, Tucker WH. 1989. *Ap. J.* 338:761–69

Rottgering HJ, Snellen I, Miley G, De Jong JP, Hanish R, Perley R. 1994. *Ap. J.* 435:654–88

Rudnick L. 2000. In *Cluster Mergers and Their Connection to Radio Sources, 24th Meet. IAU,* JD10:E22

Ruzmaikin A, Shukurov A, Sokolov D. 1987. *Magnetic Fields of Galaxies*

Ruzmaikin A, Sokolov D, Shukurov A. 1989. *MNRAS* 241:1–14

Sarazin CL. 1988. *X-Ray Emission from Clusters of Galaxies.* Cambridge, UK: Cambridge Univ. Press

Sarazin CL. 2002. In *Galaxy Clusters and the High Redshift Universe Observed in X-Rays,* ed. D Neumann, F Durret, J Tran Thanh Van. In press astro-ph/0105458

Sarazin CL. 2001b. In *Merging Processes in Clusters of Galaxies,* ed. L Feretti, IM Gioia, G Giovannini. Dordrecht: Kluwer

Schlikeiser R, Sievers A, Thiemanns H. 1987. *Astron. Astrophys.* 182:21–35

Simard-Normandin M, Kronberg PP, Button S. 1981. *Astrophys. J. Suppl. Ser.* 45:97–111

Smith E, Jones DE, Coleman PJ, Colburn DS, Dyal P, et al. 1974. *J. Geophys. Res.* 79: 3501–11

Soker N, Sarazin CL. 1990. *Ap. J.* 348:73–84

Soward AM. 1983. *Stellar and Planetary Magnetism.* New York: Gordon & Breach

Spitzer L. 1962. *The Physics of Fully Ionized Gases.* New York: Intersci.

Spitzer L. 1978. *Physical Processes in the Interstellar Medium.* New York: Wiley

Taylor GB, Allen SW, Fabian AC. 2002. *MN-RAS* Submitted astro-ph/0109337

Taylor GB, Barton EJ, Ge JP. 1994. *Astron. J.* 107:1942–52

Taylor GB, Govoni F, Allen SW, Fabian AC. 2001a. *MNRAS.* 326:2–10

Taylor GB, Inoue M, Tabara H. 1992. *Astron. Astrophys.* 264:421–27

Taylor GB, Perley RA. 1993. *Ap. J.* 416:554–62

Tribble PC. 1993. *MNRAS* 263:31–36

Turner MS, Widrow LM. 1988. *Phys. Rev. D* 37:2743–54

Vachaspati T, Vilenkin A. 1991. *Phys. Rev. D* 43:3846–55

Vallee JP, MacLeod JM, Broten NW. 1986. *Astron. Astrophys.* 156:386–90

Vallee JP, MacLeod JM, Broten NW. 1987. *Ap. J. Lett.* 25:L181–86

van Breugel WJ. 2000. *Proc. Soc. Photo-Opt. Instrum. Eng.* 4005:83–94

Vikhlinin A, Markevitch M, Forman W, Jones C. 2001a. *Ap. J. Lett.* 555:L87–90

Vikhlinin A, Markevitch M, Murray SS. 2001b. *Ap. J. Lett.* 549:L47–50

Warwick JA. 1963. *Ap. J.* 137:41–60

Waxman E, Loeb A. 2000. *Ap. J. Lett.* 545:11–14

Wentzel DG. 1974. *Annu. Rev. Astron. Astrophys.* 12:71–96

White SDM, Navarro JF, Evrard AE, Frenk CS. 1993. *Nature* 366:429–31

Willson MAG. 1970. *MNRAS* 151:1–44

Wu X-P. 2000. *MNRAS* 316:299–306

Zatsepin GT, Kuzmin VA. 1966. *Phys. JETP Lett.* 4:78–83

Zweibel EG. 1988. *Ap. J. Lett.* 329:L1–4
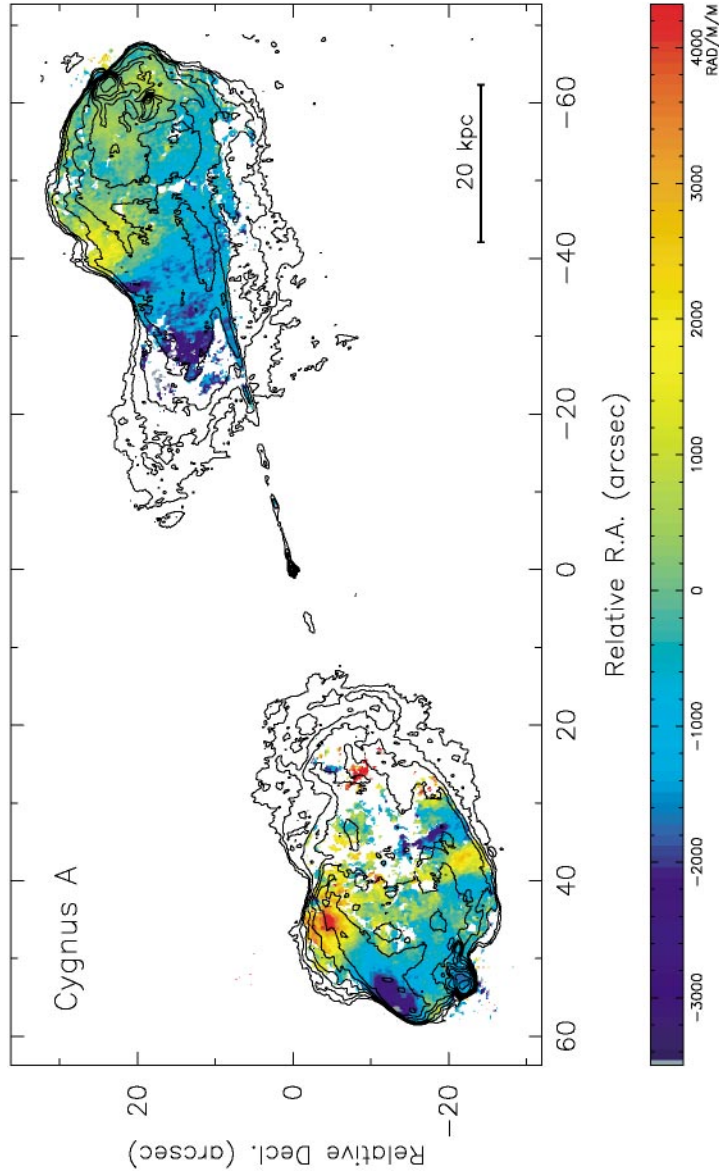
Figure 2 The RM distribution in Cygnus A based on multifrequency, multiconfiguration VLA observations. The resolution is 0.35″ (Dreher, Carilli & Perley 1987). The colorbar indicates the range in RMs from −3400 to +4300 rad m^{-2}. Note the undulations in RM on scales of 10–30 kpc. Contours are overlaid from a 5 GHz total intensity image. The RM was solved for by fitting for the change in polarization angle with frequency on a pixel-by-pixel basis (see Figure 4).
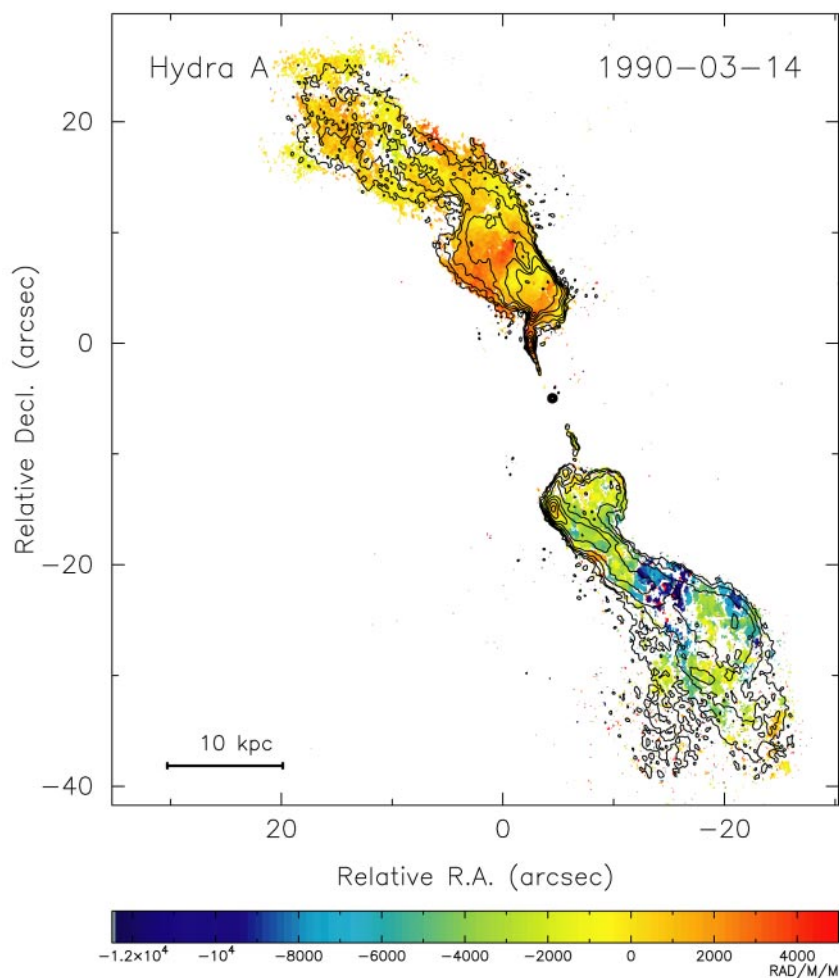
Figure 4   The RM distribution in Hydra A at a resolution of 0.3″ (Taylor & Perley 1993) with total intensity contours overlaid. Multi-configuration VLA observations were taken at four widely spaced frequencies within the 8.4 GHz band, and a single frequency in the 15 GHz band. The colorbar indicates the range in RMs from -12000 to $+5000$ rad m^{-2}. The dramatic difference in color between the lobes is due to a reversal in the sign of the magnetic field.
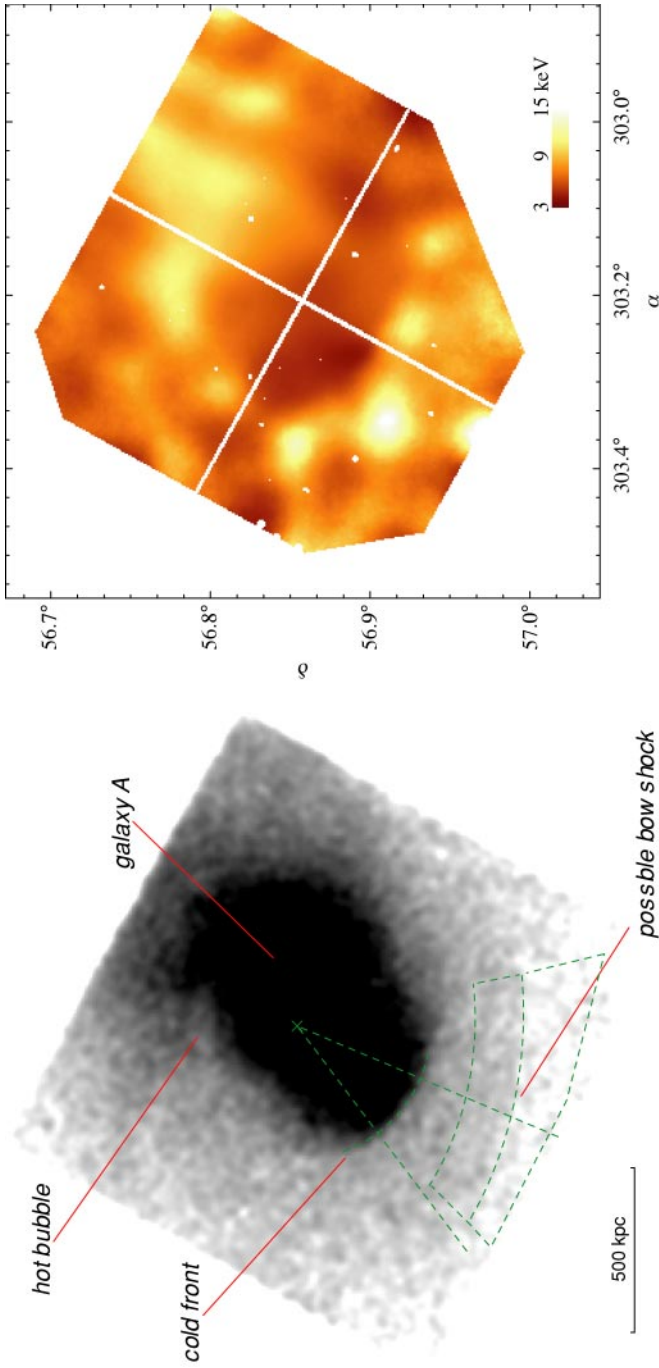
Figure 9 (*left*) A smoothed 0.5–4 keV Chandra image of Abell 3667. The most prominent feature is the sharp surface brightness edge (cold front). The front shape is nearly circular as indicated by the arc. (*right*) Temperature map. The typical statistical error in this image is ±1 keV. The cold, ∼4 keV, region near the center of the map coincides with the inside of the cold front (Vikhlinin et al. 2001a).

Annual Review of Astronomy and Astrophysics
Volume 40, 2002

CONTENTS

ERRATA
An online log of corrections to *Annual Review of Astronomy
and Astrophysics* chapters (if any, 1997 to the present)
may be found at http://astro.annualreviews.org/errata.shtml